Highly charged and stable cross-linked 4,4′-bis(4-aminophenoxy)biphenyl-3,3′-disulfonic acid (BAPBDS)-sulfonated poly(ether sulfone) polymer electrolyte membranes impervious to methanol†

Bijay P. Tripathi, Tina Chakrabarty and Vinod K. Shahi*

Received 23rd April 2010, Accepted 27th June 2010
DOI: 10.1039/c0jm01183e

Disulfonated 4,4′-bis(4-aminophenoxy)biphenyl-3,3′-disulfonic acid (BAPBDS) was synthesized as cross-linking agent. *In situ* cross-linking of sulfonated poly(ether sulfone) (SPES) *via* sulfonamide linkage was achieved using BAPBDS, for preparing polymer electrolyte membranes (PEMs), without deterioration in membrane functionality due to cross-linking. Effective cross-linking enhanced the membranes' dimensional, thermal, and chemical stability without impairing the electro-chemical properties such as ion-exchange capacity and proton conductivity. Thus, the properties of the developed PEMs were significantly improved due to more compact structure of the cross-linked SPES membrane (CPES) over membranes without crosslinking. Comparable selectivity parameter (*SP*) and direct methanol fuel cell (DMFC) performance of the developed membranes, especially CPES-100, with Nafion 117 (N117) indicated their suitability for fuel cell applications.

Introduction

Modern energy conversion technologies such as proton-exchange membrane fuel cells (PEMFCs) and/or direct methanol fuel cells (DMFCs) are interesting applications for ion-conducting membranes.[1–4] DMFCs were pushed toward the brink of commercialization which offered the potential for long lifetimes, ability to refuel and operation at moderate temperature.[5–7] Generally, perfluorosulfonic acid PEMs such as Nafion (developed by DuPont) are reference membranes for DMFC because of their high electrochemical properties as well as excellent chemical stability.[8–10] However, there is much interest in alternatives to PEMs because of the reduced performance of Nafions above 80 °C, high methanol crossover, and cost.[8,9] Consequently, there is a demand for developing novel thermally and chemically stable PEMs as an alternate of perfluorinated polymer electrolyte with low methanol crossover, cost and improved processability.[10–14]

PEMs based on aromatic hydrocarbon polymers such as poly(ether ether ketone)s,[15–17] poly(arylene ether sulfone)s,[18] polyimides,[19–21] polyphosphazenes,[22] polybenzimidazoles,[23] and polyphenylenes[24] were extensively studied due to their excellent stability and easy functionalization.[25] Thermally and environmentally stable SPES was indentified as promising material for PEMs application. However, high extent of sulfonation was required to achieve sufficient proton conductivity. But, high sulfonation level results excessive membrane swelling (even soluble in methanol–water solution) and loss in mechanical properties.[26] Cross-linking is an attractive method for researchers to reduce the swelling and mechanical instability problems. Reports are available where cross-linking was employed to obtain highly functionalized PEMs with reasonable swelling and without impairing other properties.[27–31] These cross-linked membranes with low swelling and methanol crossover showed deterioration in membrane conductivity with increase in cross-linking extent, because consumption of sulfonic acid groups. Nolte *et al.*[32] reported a versatile *in situ* cross-linking technique for SPES using diamine as cross-linking agent to circumvent this deterioration. But reduction in conductivity and permselectivity due to crosslinking was observed because of loss in fixed charges ($-SO_3H$) during conversion of sulfonic acid groups into sulfonamide groups. Recently, Na and coworkers[33] reported cross-linked sulfonated poly(ether ether ketone) (SPEEK)-benzimidazole membrane. But, cross-linking of SPEEK with carboxyl-terminated benzimidazole consumed two sulfonic acid groups per monomer, which reduced membrane functionality and conductivity. Thus, a novel cross-linking agent is highly required to circumvent the deterioration in membrane functionality and conductivity due to cross-linking.

Herein, we propose a new strategy for the synthesis of cross-linking agent (BAPBDS) for developing highly stable and functionalized PEMs without any deterioration of functional groups or membrane conductivity due to cross-linking. We prepared BAPBDS-SPES cross-linked membranes for fuel cell applications. Prepared membranes were extensively evaluated in terms of water uptake, types of water, water retention capacity, swelling ratio, proton conductivity and methanol permeability. Results demonstrated that reported method of cross-linking is suitable for tailoring cross-linked aromatic thermoplastic PEM for future electro-membrane and fuel cell applications.

Electro-Membrane Processes Division, Central Salt & Marine Chemicals Research Institute, Council of Scientific & Industrial Research (CSIR), G. B. Marg, Bhavnagar, 364002, Gujarat, India. E-mail: vkshahi@csmcri.org; vinodshahi1@yahoo.com; Fax: +91-278-2567562/2566970; Tel: +91-278-2569445

† Electronic supplementary information (ESI) available: Solvent uptake studies; water retention studies; ion-exchange capacity (IEC) measurements; dimensional, oxidative and hydrolytic stabilities; membrane conductivity measurement; methanol permeability measurements; and solubility of the cross-linked membrane. See DOI: 10.1039/c0jm01183e

Experimental section

Materials

Poly(ether sulfone) (PES), 1,1′-carbonyl-diimidazole (CDI), 4,4′-bis(4-aminophenoxy)biphenyl (BAPB), and Nafion117 (perfluorinated) membrane were obtained from Sigma-Aldrich Chemicals and used as received. H_2SO_4, HCl, H_2O_2, NaOH, NaCl, $FeCl_3$, dimethylacetamide (DMAC), methanol and ethanol of AR grade were received S.D. Fine Chemicals, India. Aniline (AR grade, S.D. Fine Chemicals, India) was distilled prior to use. Double distilled water was used for all purposes.

Synthesis of BAPBDS

To a 100 ml three-neck flask, equipped with a mechanical stirring device, 11.0 g (30 mmol) of BAPB was added. In cooled (ice-bath) flask 18 ml of concentrated sulfuric acid was slowly added under constant stirring. The mixture was continuously stirred at 0 °C for 30 min followed by slight heating until the BAPB was dissolved. 4.2 ml of fuming sulfuric acid (60% SO_3) was slowly added to the cooled mixture and under stirring (30 min.) at 0 °C and for 2 h at 50 °C. Reaction mixture was cooled to room temperature and poured into crushed ice. Filtered off solid was dissolved in NaOH solution. Filtrate was acidified with concentrated hydrochloric acid. Precipitate was washed with de-ionized water, methanol, and dried at 90 °C in vacuum. IR spectrum (KBr, cm^{-1}): 3405, 2967, 1626, 1544, 1467, 1376, 1248, 1170, 1090, 1019, 880, 848, 830, 743, 703, 670, 614, 580, 535. ^{1}H NMR spectrum (in DMSO-*d*6 in the presence of a drop of Et_3N for dissolution of BAPBDS): 8.04, 7.62, 7.25, 6.9, 4.57, and 2.53. ^{13}C NMR spectrum: 155.76, 164.26, 145.36, 136.53, 132.28, 126.6, 121.69, 117.8, and 115.43 (detailed peak assignments for ^{1}H and ^{13}C NMR are also given in Fig. S1 and S2 in the ESI†). Elemental analysis (CHNS): Calculated for $C_{24}H_{20}N_2O_8S_2$: C, 54.54; H, 3.81; N, 5.30; S, 12.12. Found: C, 52.06; H, 4.20; N, 4.98; S, 11.05.

Sulfonation of PES and the membrane preparation

Sulfonation of PES was carried out as reported earlier[34] using conc. H_2SO_4 (95–98%) under vigorous stirring at 40 °C for 24 h. The precipitated polymer was filtered, washed with distilled water until only a trace of acid remained and dried under vacuum for 12 h at 80 °C. About a 58–60% degree of sulfonation was determined by ion-exchange capacity, elemental analysis and ^{1}H-NMR.[32]

The cross-linking procedure for SPES has been described in Scheme 1. The sulfonic acid groups were activated by CDI and yielded *N*-sulfonyl-imidazole. Neutralization of imidazole with sulfonic acid groups resulted into salt formation. After the addition of sulfonated diamine (BAPBDS), the color of the solution mixture changed to brownish. After continuous stirring at room temperature (6 h), the obtained viscous solution was transformed into thin film on a clean glass plate. The membranes were dried under IR lamps and cured at 60 °C under vacuum for 12 h. Thus obtained flexible, brownish, and transparent membranes were conditioned with 0.1 M NaOH for 12 h, rinsed with double deionized water and further with 0.1 M HCl followed by repeated washing with water. Finally the membranes were stored in double deionized water. The obtained membranes were designated as CPES-X, where X is the weight percentage of BAPBDS to the SPES (where X is 0, 25, 50, 75, and 100).

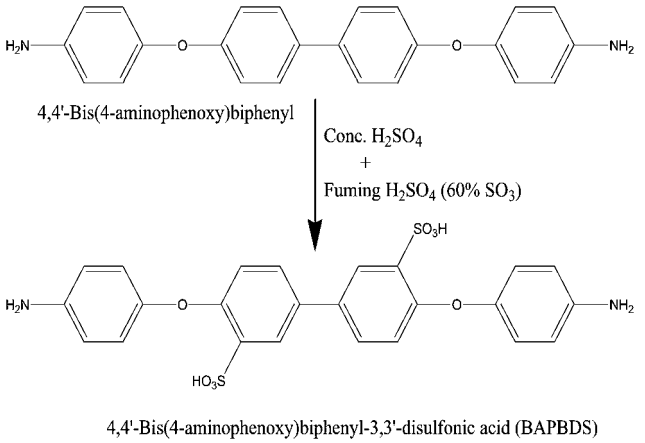

Scheme 1 The sulfonation process for 4,4′-bis(4-aminophenoxy)biphenyl.

Instrumental characterization of the membranes

^{1}H NMR of BAPBDS was recorded in DMSO-d_6 in the presence of a drop of Et_3N for dissolution by NMR spectrometer (Brüker, 200 MHz), and the FTIR was obtained by KBr pellet method. FT-IR spectra of completely dried membrane samples were recorded using ATR technique with spectrum GX series 49387 spectrometer in the range of 4000–600 cm^{-1}. Elemental analysis of the BAPBDS was carried out using Perkin-Elmer-2400 CHNS analyzer.

Thermal degradation and stability of the membranes were investigated by thermogravimetric analyzer (TGA) (Mettler Toledo TGA/SDTA851^e with star^e software) in nitrogen atmosphere at a heating rate of 10 °C min^{-1} from 50 to 600 °C. Differential scanning calorimetry (DSC) measurements were carried out in a temperature range of 50 to 400 °C. The samples of about 10 to 20 mg were loaded into aluminium pans, and then heated to the desired temperature at a heating rate of 5 °C min^{-1}. The empty aluminium pan was used as a reference during the course of experiment.

Scanning electron microscopy (SEM) images of the dried membranes were recorded using a LEO Instruments (Kowloon, Hong Kong) microscope after gold sputter coatings on desired membrane samples.

Physicochemical and stability analysis

Solvent uptake of membrane was recorded in equilibrium with water or water–methanol mixture (30% methanol). Procedures for the determination of solvent uptake and number of water molecules per ionic site are included in the ESI (S1).† For the determination of bound water content, wet membrane samples were heated in a TGA at a rate of 10 °C min^{-1} under nitrogen atmosphere and the weight loss percentage of the membrane (100–150 °C) was calculated.[35,17] The water retention ability of the developed membranes was evaluated by measuring water mobility during the dynamic deswelling test.[36–38] The detailed procedure is given in the ESI (S2).† The ion exchange capacity

(IEC) was measured by the classical titration method as reported previously[39,40] and included in the ESI (S3).† Dimensional, oxidative and hydrolytic stabilities of the membranes were examined and detailed procedures are given in the ESI (S4).[40]†

Membrane conductivity and methanol permeability

Membrane conductivity of hydrated cross-linked membranes was measured by potentiostat/galvanostat frequency response analyzer (Auto Lab, Model PGSTAT 30). The detailed procedure is given in the ESI (S5).† Methanol permeability of the composite membranes was determined in a diaphragm diffusion cell and the procedure is described in the ESI (S6).†

Membrane electrode assembly (MEA) and DMFC testing

Gas diffusion electrodes with three-layer structure were prepared by the method reported earlier in literature.[36,39] Preparation method includes: (i) wet proofing of carbon paper (Toray Carbon Paper, thickness: 0.27 mm); (ii) coating of gas diffusion layer (GDL) on to the carbon paper; (iii) coating of catalyst layer on to the GDL. The carbon paper was wet proofed with 15 wt% PTFE solution by brush painting method. The GDL (25 cm^2 geometric area) was fabricated by coating slurry of 0.95 mg cm^{-2} consisting of carbon black (Vulcan XC72R) and PTFE dispersion on carbon paper. The anode was made by coating a slurry of catalyst (20 wt% Pt + 10 wt% Ru on carbon), 5 wt% Nafion ionomer solution, isopropanol, and Millipore water (catalyst ink) on GDL had a loading of 1 mg Pt and 0.5 mg Ru. While the cathode was obtained by coating the same catalyst ink lacking Ru with same loading. Electrodes were cold pressed with membrane and cured at 60 °C for 12 h, followed by hot pressing at 130 °C for 3 min at 1.2 MPa. The MEA was achieved by hot pressing an electrode/membrane/electrode sandwich at 100 °C for 3 min at 1.0 MPa. The MEA was clamped in single cell (FC25-01 DM fuel cell).

The current–voltage polarization curves were recorded with the help of MTS-150 manual fuel cell test station (ElectroChem Inc., USA) with controlled fuel flow, pressure and temperature regulation attached with electronic load control ECL-150 (ElectroChem Inc., USA). The measurements were performed in the air mode of operation at 10 psi pressure with a fixed concentration of methanol fed at the anode side with pressure 7 psi at 70 °C for a representative membrane.

Results and discussion

Synthesis of BAPBDS and preparation of cross-linked membranes

BAPBDS was synthesized by direct sulfonation of BAPB (Scheme 1) with conc. H_2SO_4 and consequently with fuming H_2SO_4 (60% SO_3) at 50 °C. Sulfonation occurred only at 3,3′-positions, because of high electron density and thus reactive nature of central phenyl rings. Terminal phenyl rings (to which amino groups were attached) were less reactive due to the strong electron-withdrawing effect of the protonated amine groups. ^1H and ^{13}C NMR (Fig. 1 (A and B)) and IR spectra (Fig. 2) confirmed the chemical structure of the product. The elemental analysis also supported the information revealed by spectroscopy.

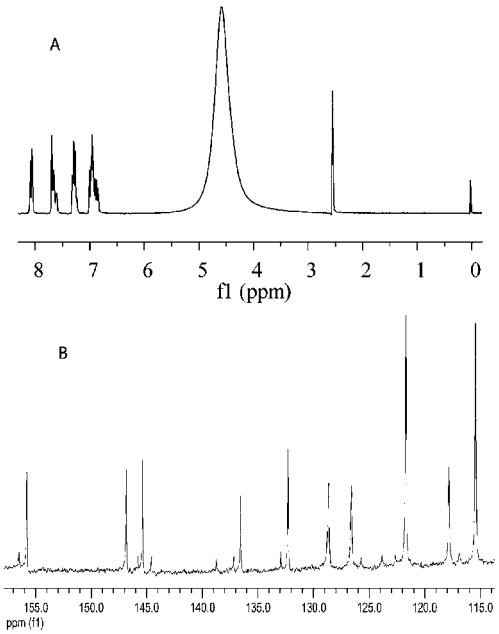

Fig. 1 NMR spectra of sulfonated diamine (BAPBDS): (A) ^1H NMR; (B) ^{13}C NMR spectrum.

SPES (58–60% degree of sulfonation) was dissolved in DMF and several cross-linked SPES membranes were prepared using BAPBDS. After the activation of sulfonic acid groups (SPES) by CDI, BAPBDS was added to the solution. Covalently bonded imidazole moiety was replaced by BAPBDS. Thus, two SPES chains were cross-linked with BAPBDS without the loss of net sulfonic group concentration in the membrane. Activation of sulfonic acid group is necessary for covalent cross-linking (crosslinking between BAPBDS and SPES). However, there was also possibility of ionic cross-linking between the BAPBDS and SPES at higher BAPBDS concentration. At high BAPBDS content, there was possibility for reaction of only one amine group with SPES chain. The schematic structure of cross-linked membrane is presented in Scheme 2.

The structure of the cross-linked membranes was confirmed by ATR-FTIR spectroscopy presented in Fig. 2 (representative spectrum of CPES-50). The aromatic C–C stretching vibration was observed at 1578 and 1478 cm^{-1} with sharp to medium intensity peaks at 2000–1800 cm^{-1}, which are characteristic of 1,2-disubstituted and 1,2,4-trisubstituted aromatic moieties.[41] All membranes show a strong –SO_3H stretch at ~1100 (sym. SO_3 stretch), ~1239 (asym. SO_3 stretch), ~2368–1650 (due to the –OH stretching vibration) cm^{-1}, which confirmed the presence of sulfonic acid group.[41] The cross-linking was confirmed due to the presence characteristic peaks of secondary sulfonamide group.[42] A strong band at 3235 cm^{-1} showed the presence of N–H groups, while another at 1150 cm^{-1} was due to the symmetric stretching vibration of SO_2 groups in the solid phase. Slight increases in SO_2 group frequencies were observed due to the bonding with electronegative nitrogen atom.[42]

Morphology of the cross-linked membranes

SEM images for cross-linked CPES-X membranes are depicted in Fig. 3. Uncross-linked membrane (CPES-0) was transparent

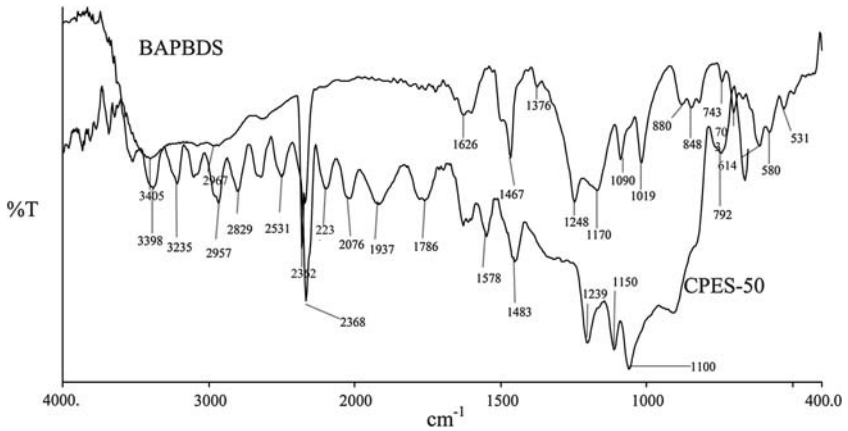

Fig. 2 FTIR spectra of sulfonated diamine BAPBDS and a representative crosslinked sulfonated poly(ether sulfone) (CPES-50).

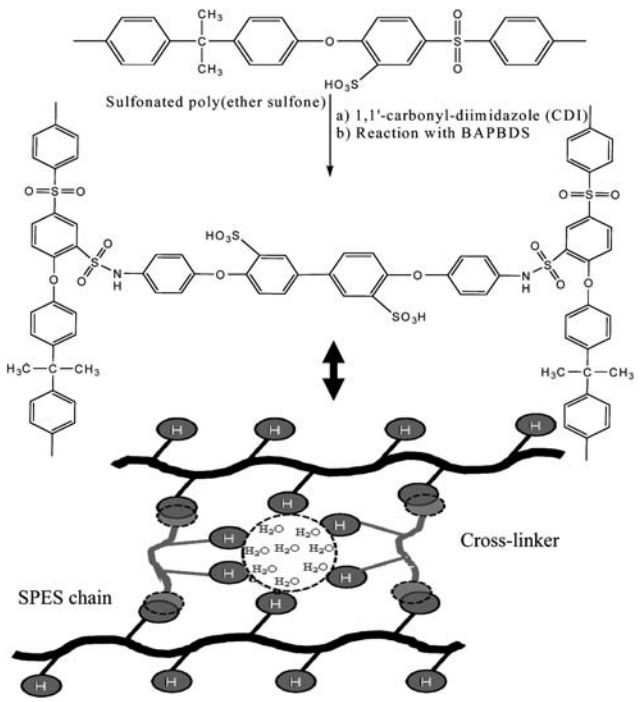

Scheme 2 The schematic structure of cross-linked sulfonated poly(ether sulfone).

and more flexible than cross-linked membranes. With the increase in cross-linking agent (diamine) content, brownish membranes turned deep brown. The prepared membranes were dense in nature without any holes or cracks (Fig. 3 (A, B, and C)). However, slightly rough surface was observed at high cross-linker concentration.

Thermal characterizations

The thermal degradation stability of the membranes (in H^+ form) was analyzed by TGA (Fig. 4). TGA curves showed three-step weight loss. The initial weight loss aroused due to absorbed water in the polymer matrix. In this region, maximum weight loss for uncross-linked SPES membrane (CPES-0) was attributed to its high water uptake. For CPES-0 membrane, loss of bound and hydrated water was higher than cross-linked membrane, because of more absorbed/bulk water. After cross-linking, comparatively less space was available to accommodate the bulk water. The second degradation step was started at around 250–300 °C and is attributed to the loss in the sulfonic acid groups.[43] The third weight loss (beyond 450 °C) aroused due to degradation of the polymer matrix. These results indicated thermal stability of the developed membranes under DMFCs operating conditions. Fig. 5 (DSC thermograms) showed slow increase in T_g value (3–4 °C) with cross-linking density for CPES-X membranes.

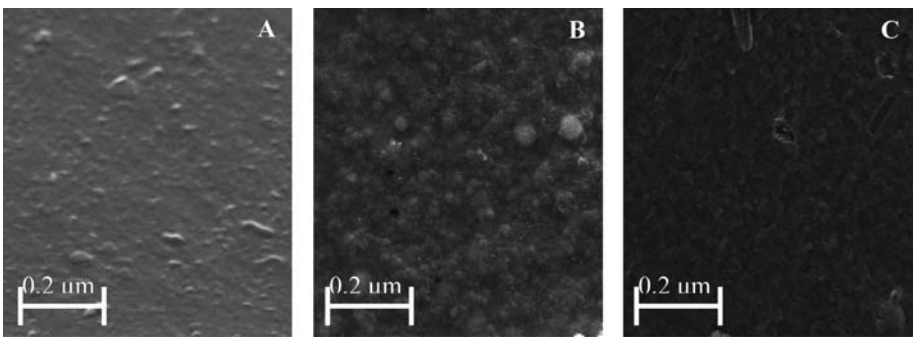

Fig. 3 SEM images of polymer electrolyte membranes: (A) CPES-0; (B) CPES-50; and (C) CPES-100.

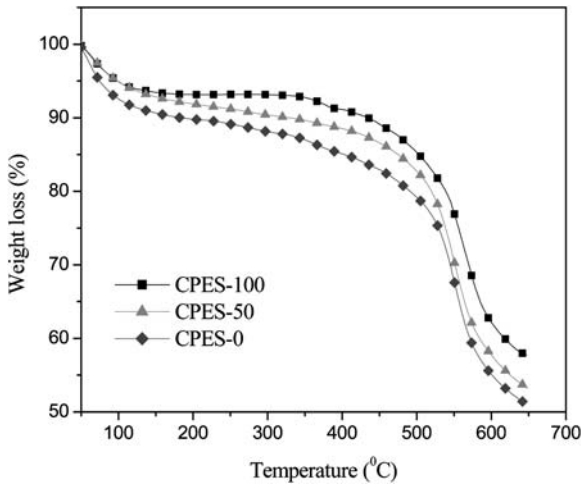

Fig. 4 TGA thermograms of all developed polymer electrolyte membranes.

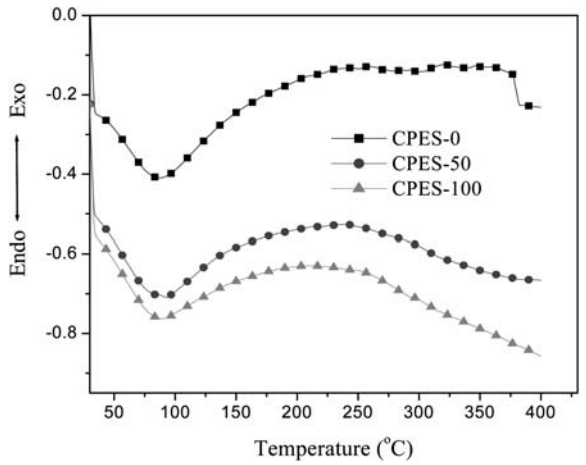

Fig. 5 DSC thermograms of the developed polymer electrolyte membranes.

After the cross-linking, polymer chains became more compact and stiff.

Solvent uptake, stability and solubility studies

The water uptake of polymers has a profound effect on proton conductivity, mechanical, and dimensional properties.[44] The presence of water molecules in the membrane matrix facilitates the dissociation of functional groups and proton transport. However, excessive water uptake deteriorated membrane mechanical properties and dimensional stability. Water and water–methanol uptake values for different membranes are presented in Table 1 and Fig. 6. The solvent uptake character of the membranes was reduced with cross-linking density. Water absorption occurs due to the presence of functional groups (–SO_3H in this case) and thus hydrogen bonding, through which water accommodated in the space between polymer chains. Cross-linking hindered mobility of polymer chains and reduced the void space responsible for water and water–methanol uptake. BAPBDS unit associated with highly cross-linked structures, and imposed restriction on the mobility of polymer chains. The effect of temperature on solvophilicity was also performed and water uptake was increased with temperature. This variation was attributed to the membrane swelling and easy penetration of water molecule into the swelled polymer matrix. Developed membranes were more solvophilic in water–methanol (50%) mixture. The water–methanol uptake was high in compare with water uptake. However, solvent uptake nature of the developed membranes was similar to N117 membrane.

Proton transport in N117 membrane proceeds through the ionic cluster regions in the membrane phase.[45] Functional groups contribute to the formation of ionic clusters filled with associated water (bound and unbound water). The number of water molecule per ion-exchangeable group (λ_w) is depicted in Table 1. Membrane with larger and/or numerous ionic cluster regions showed advantage for proton transport. In addition, size and/or number of ionic clusters depend on the water content and IEC of the membrane. λ_w values for prepared cross-linked membranes were smaller than uncross-linked and N117 membrane. Thus, the developed composite membrane may be classified as "*water poor*". The presence of additional water enhanced proton mobility and conductivity. Larger ionic clusters presumably reduced the extent of ionic interaction between proton conducting channels and thus enhanced the proton mobility.

Extreme swelling and dimensional instability in methanol–water, especially at high temperature, is a distinct disadvantage of most of the sulfonated hydrocarbon based PEMs. High methanol concentration also caused excessive dimensional and surface area change, responsible for uneven stresses between membrane and electrodes during sealing of the membrane electrode assembly. The degree of swelling of the membranes was estimated in terms of change in volume fraction in water and water–methanol mixture (50%) and results are depicted in Table 1. Membrane swelling was high in water–methanol mixture. Considerable reduction in volume expansion was observed due to high cross-linking density. This phenomenon can be explained on the basis of increased interactions of the polymer molecules and restrained movement of polymer chains after cross-linking. Therefore, cross-linking effectively improved the dimensional stability of the membranes.

The membranes' oxidative stability under PEMFC operating conditions is essential due to formation of H_2O_2, $^{\bullet}OH$, and $^{\bullet}OOH$ radicals during water splitting, which believed to attack on hydrogen containing. Membrane stability in strong oxidative conditions was evaluated in Fenton's reagent (3% aq. H_2O_2 + 3 ppm $FeSO_4$) and results are included as oxidative weight loss percent (W_{OX}) in Table 1. CPES-100 membrane showed highest oxidative stability. After cross-linking the hydrophilic domains became compact and because of very short life time of $^{\bullet}OH$ or $^{\bullet}OOH$ radicals, they cannot penetrate inside the domains. All synthesized PEMs retained more than 95% weight after oxidative experiments, showed better stability after cross-linking.

Developed membranes were also subjected to accelerated hydrolytic stability testing at 140 °C and 100% RH for 24 h. Membranes retained their transparency, flexibility and toughness. High weight loss of these membranes under hydrolytic conditions (W_{HS}) (Table 1) was attributed to hydrolysis of the sulfonamide linkage in the cross-linked membrane.

Table 1 Water uptake (φ_w), water–methanol uptake (φ_{w+MeOH}), number of water molecules per ionic sites (λ_w), change in volume fraction in water (Φ_W), change in volume fraction in methanol (Φ_M), oxidative and hydrolytic weight loss (W_{OX} and W_{HS}, respectively), and water diffusion coefficient (D) values for different membranes

Membrane	φ_w (wt %)	φ_{w+MeOH} (wt %)	λ_w	Φ_W	Φ_M	W_{OX} (wt %)	W_{HS} (wt %)	$D/10^{-7}$/cm^2 s^{-1}
CPES-0	26.84	28.74	12.96	0.36	0.42	6.24	5.37	6.76
CPES-25	26.38	26.96	11.10	0.31	0.38	5.18	7.24	6.23
CPES-50	25.66	25.30	10.48	0.28	0.35	4.33	7.96	4.64
CPES-75	22.85	24.62	9.00	0.25	0.31	4.08	8.20	3.99
CPES-100	22.14	24.35	8.37	0.24	0.29	3.91	8.61	4.39

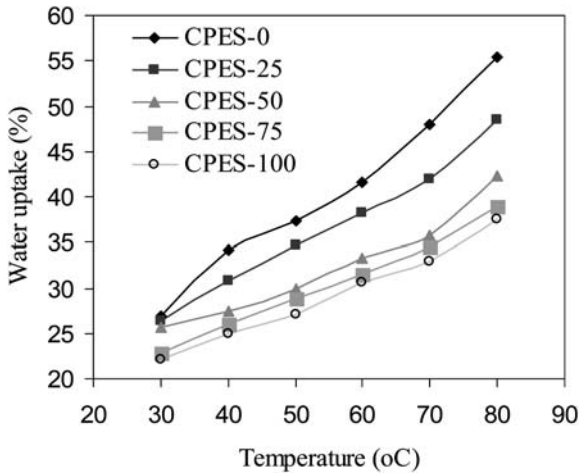

Fig. 6 The effect of temperature on total water uptake values.

Solubilities of PES, SPES, and CPES-100 membrane were also tested in different organic solvents at RT and in water under boiling conditions and the data are given as ESI (section S7).† All three were soluble in selected polar aprotic solvent. In case of water, both SPES and CPES-100 showed high swelling. Furthermore, both are partially soluble in methanol.

State of water and water retention ability

According to the Eikerling's theory,[46] PEMs posses two types of water: bound water and the bulk water. Bound water required for the solvation of the sulfonic acid groups, while bulk water fills the void volume. The bound water was estimated by TGA,[47] and bulk water was obtained by subtracting the bound water content from the total water content of the membranes. For easy comparison, weight loss percentages for membrane samples were fixed 100% at 100 °C (ESI Fig. S3†). CPES-0 membrane showed lowest water retaining ability with low bound water content (1.489%) in compare with CPES-100 membrane (1.954%) (Table 2). Relatively less cross-linked membrane showed slightly high bound water content. High total/bulk/bound water content of these membranes improved their water retaining ability and thus proton conductivity under low humid conditions.

Water vapor sorption and diffusion properties of PEMs have significant effect on their conductivity and thus PEMFC applicability. The water retention capability of cross-linked membranes was illustrated in Fig. S4 (A) (ESI)† by (M_t/M_o)–t (time) curves. The deswelling kinetics of the developed membranes was further characterized by plotting $(M_t/M_0$–$t^{1/2})$ curve (Fig. S4 (B) ESI†) using following equation, derived from Higuchi's model:[38]

$$M_t/M_o = -kt^{1/2} + 1 \quad (1)$$

where M_o and M_t is the initial amount of water and water remaining in polymer matrix at any given time, and k is a constant.

The obtained straight lines for varying BAPBDS content fitted to Higuchi's model, and suggested a diffusion controlled water desorption mechanism. Because of enhanced cross-linking, the rate of water desorption was reduced with BAPBDS content. Thus, BAPBDS acted as water binder in the membrane matrix due to the formation of highly cross-linked SPES chains. Cross-linking was responsible for the formation of water filled ionic clusters, as shown in Scheme 2. Free water was more bound in nature with inter polymer chains and less opt to dehydration. Water diffusion coefficient (D) for all the membranes was also evaluated from a best-fit normalized mass change and depicted in Table 1. The diffusion coefficient decreased significantly with BAPBDS content in the membrane matrix. Thus, BAPBDS acted as barrier for water release and improves the water retention capacity even at higher temperature.

Ion-exchange capacity and proton conductivity

The IEC depends on the density of functional groups and plays an important role in water uptake and proton conductivity. The

Table 2 Total, bulk, and bound water content of cross-linked polymer electrolyte membranes

Membrane	Total water (%)	Bulk water[a] (%)	Bound water[b] (%)
CPES-0	26.84	25.35	1.489
CPES-25	26.38	23.99	2.384
CPES-50	25.66	23.55	2.107
CPES-75	22.85	20.94	1.901
CPES-100	22.14	20.18	1.954

[a] Bulk water = total water – bound water. [b] Bound water was determined by percent weight loss in TGA between 100 to 150 °C temperatures.

Table 3 Ion-exchange capacity (IEC), proton conductivity (κ^m), methanol permeability (P) and energy of activation (E_a) values for different membranes compared with Nafion117 membrane

			$P/10^{-7}$ cm^2 S^{-1}		
Membranes	IEC/mequiv. g^{-1}	$\kappa^m/10^{-2}$ S cm^{-1}	30% (MeOH–water)	50% (MeOH–water)	E_a kJ mol^{-1}
CPES-0	1.15	1.63	3.33	8.14	8.85
CPES-25	1.32	1.83	0.74	6.66	9.06
CPES-50	1.36	1.97	0.76	4.58	9.65
CPES-75	1.41	2.19	0.77	2.15	10.02
CPES-100	1.47	2.64	0.65	2.02	10.81
N117	0.90	9.56	13.10	—	6.14

IEC values (Table 3) increased with BAPBDS content. During cross-linking, consumption of two –SO_3H groups was compensated by BAPBDS (it contains two –SO_3H groups). An increase in IEC may be attributed to the increase in density of functional groups due to enhanced compactness of the matrix by cross-linking. Among the prepared membranes, the CPES-100 membrane showed 1.47 mequiv. g^{-1} IEC, higher than N117 membranes (0.90 mequiv/g).

Acidic functional groups (–SO_3H) of cross-linked PEMs dissociated due to hydration and allowed the transport of hydrated protons (H_3O^+). The proton conductivity was measured from 30 to 80 °C for hydrated membranes, and relevant data are presented in Table 3. It was noticed that an increase in BAPBDS content enhanced the proton conductivity. The CPES-100 membrane showed highest conductivity (2.64×10^{-2} S cm^{-1}). Conductivity of PEMs arose due to the presence of functional groups and hydrophilic proton conductive channels (ionic clusters).[48] An increase in bound water percent with BAPBDA content also affected the proton conductivity. Formation of sulfonamide linkage (with active hydrogen on nitrogen), which acted as proton acceptors and behaved like a sink for H^+, which supported its fast dissociation and propagation. CPES membranes showed 9.06–10.81 kJ mol^{-1} activation energy (Table 3), which suggested Grotthuss proton transport mechanism. Proton transport occurred through –SO_3H groups, presented in crosslinked membrane matrix. The cross-linked structure created water filled ionic clusters/channels surrounded by sulfonic and sulfonamide groups (Scheme 2). The proton transport through membrane occurred by its exchange between sulfonic acid groups *via* sulfonamide groups. Thus proton transport was facilitated by the existence of ionic clusters/channels, which may be responsible for easy proton transport and high conductivity. Earlier report showed deterioration in conductivity due to cross-linking (serious drawback of cross-linking).[32] But, in this report (CPES membranes) conductivity was maintained in spite of cross-linking (compensated by addition of BAPBDS). Simultaneously, conductivity of N117 membrane was found to be 9.56×10^{-2} S cm^{-1} under similar experimental conditions.

Membrane conductivity data at elevated temperatures (30 to 80 °C) under 100% RH are presented as Arrhenius plot (Fig. 7) for the estimation of activation energy (E_a) required for proton transport across the membrane. Conductivity followed Arrhenius behavior and activation energy was obtained by following equation:

$$E_a = -b \times R \quad (2)$$

where b is the slope of the regression line of $ln\kappa^m$ (S cm^{-1}) *vs.* $1000/T$ (K^{-1}) plots and R is the gas constant (8.314 J K^{-1} mol^{-1}). CPES membranes showed positive temperature-conductivity dependencies (Table 3). This observation suggested thermally activated conduction process. E_a values increased with BAPBDS content (8.85–10.81 kJ mol^{-1}), while CPES-0 membrane showed comparable E_a value with N117 membrane (6.52 kJ mol^{-1}).[36] Inter-linked and continuous hydrophilic channels were responsible for fast ion/molecule diffusion and rapid conduction, at high temperature.

Methanol cross-over and selectivity parameter

Methanol cross-over from anode to cathode reduces energy efficiency, cathode voltage, and increases thermal load on DMFC cell. The methanol permeability profile for all prepared membranes was assessed for 30 and 50% (v/v) methanol–water and the relevant data are presented in Table 3. Methanol permeability coefficients for these membranes were lower in comparison with N117 membrane (13.10×10^{-7} cm^2 s^{-1}). Relatively less pronounced hydrophobic/hydrophilic separation of sulfonated aromatic polymers in comparison with Nafion resulted in narrow and/or less connected hydrophilic channels and low methanol permeability.[49] Methanol permeability decreased with BAPBDS content and thus cross-linking density in the membrane matrix. Highly cross-linked membrane (CPES-100)

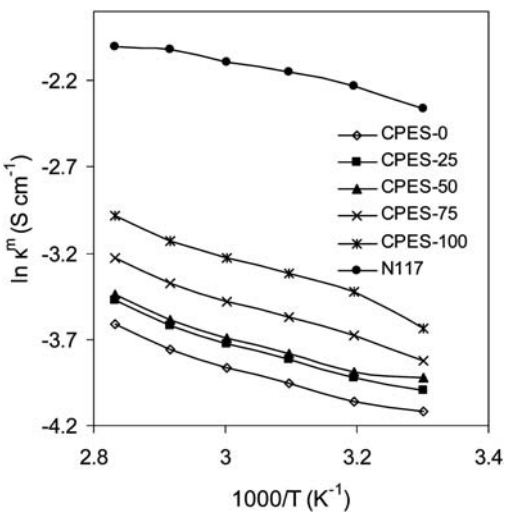

Fig. 7 Arrhenius plot in 100% RH environment, for different developed proton exchange membranes.

showed five-times lower methanol permeability than uncross-linked (CPES-0). The permeation of liquid/gas molecules through the polymer membrane occurs *via* diffusion mechanism, and the permeability of the penetrant (methanol in this case) is the product of its solubility and diffusivity. The penetrant diffusivity is dependent on the free void volume in the membrane matrix, the size of the penetrant molecules, and segmental mobility of polymer chain. Cross-linking effectively suppressed the size of the hydrophilic channels, and thus inhibited the methanol permeability. Methanol dominantly permeates by hopping between ionic sites through hydrophilic channels along with proton. Thus the methanol permeability strongly depends on the size of the ionic channels and tortuousity of proton conducting path.

To directly compare the applicability of the developed cross-linked PEMs for DMFC application, ratio of proton conductivity and methanol permeability (κ^m/P) data were used as selectivity parameters (SPs). SP values for cross-linked and N117 membranes are presented in Fig. 8. CPES-100 membrane exhibited highest SP value (4.056×10^5 and 7.79×10^5 S cm^{-3} s at 30 and 80 °C respectively) among the prepared membrane. The SP value linearly increased with BAPBDS content in the membrane matrix. Under similar conditions N117 membrane showed 0.72×10^5 and 1.019×10^5 S cm^{-3} s SP value at 30 and 80 °C respectively. It was also noticed that SP values for cross-linked membranes were increased with temperature. This observation may be attributed to relatively low methanol permeability and high conductivity of the prepared membranes. These results can be explained on the basis of the lack of significant interactions between methanol and functional groups. Ionized groups hydrate strongly and excluded organic solvents (salting-out effect), which is an essential feature of the polyelectrolyte membranes. Furthermore higher SP values of these membranes indicate great advantage for DMFC applications.

DMFC performance studies

DMFC performance for developed PEMs was tested in a single cell in comparison with N117 membrane. Fig. 9 showed the polarization curves (current density as a function of cell potential and power density) for CPES-0, and CPES-100 and N117 in a DMFC at 70 °C. Studied PEMs showed 0.45 V open circuit voltage (OCV). The current densities at a potential of 0.20 V for CPES-0, CPES-100 and N117 (43.30, 53.24 and 45.1 mA cm^{-2}, respectively) indicated the comparable DMFC performance of CPES-100 and N117 membrane. Good performance of the CPES-100 membrane was observed due to extremely low methanol permeability in spite of its lower proton conductivity. CPES-100 showed 10.72 mW cm^{-2} maximum power density, whereas for N117 it was about 9.25 mW cm^{-2}. These results indicated improved performance of cross-linked SPES membranes in compare with N117 membrane.

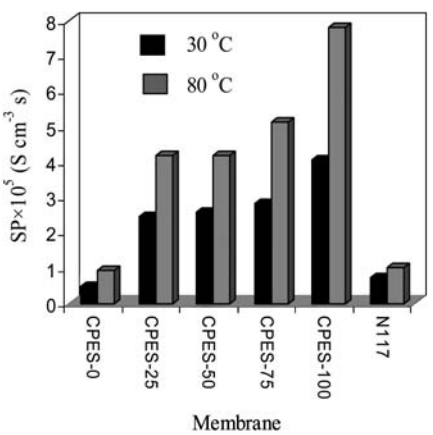

Fig. 8 Selectivity parameter values for different membranes at 30 and 80 °C temperature.

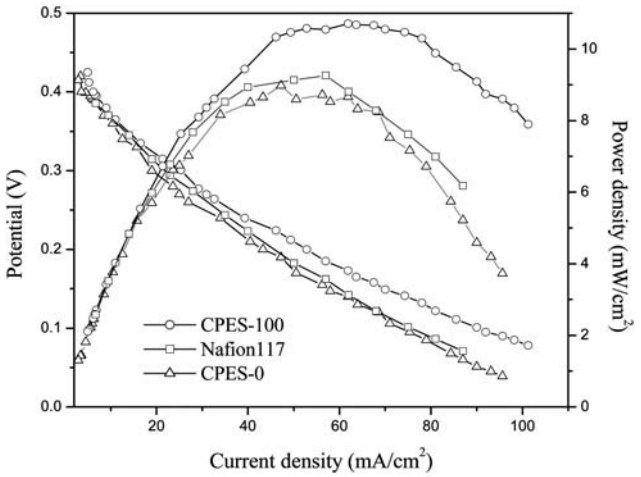

Fig. 9 DMFC performance curves for MEAs made with different membranes operated at 343 K for 25% (v/v) methanol used as fuel in air mode with 10 psi pressure.

Conclusions

A novel cross-linking agent (BAPBDS) was synthesized and the preparation procedure for cross-linked SPES membranes was reported. Previously studied cross-linking methodologies showed deteriorative effect on membrane functional group concentration and conductivity. Cross-linking using BAPBDS, improved membrane functionality, conductivity, stability and reduced swelling characteristics. The sulfonation of cross-linking agent (BAPBDS) was confirmed by elemental analysis, FTIR, and NMR techniques. Solution cross-linking of SPES with BAPBDS was achieved by activating the sulfonic acid groups with CDI, at room temperature. The cross-linked membranes were characterized for different physicochemical and electrochemical properties in comparison with N117, for DMFCs applications. The physicochemical and electrochemical properties of prepared membranes were highly dependent on BAPBDS content. Developed membranes showed good stabilities, flexibility, water uptake, and water retention capacities. Among the developed membranes, CPES-100 exhibited high IEC value (1.47 mequiv./g), proton conductivity (2.64×10^{-2} S cm^{-1}), and lowest water uptake (22.85%) and methanol permeability (0.65×10^{-7} cm^2 S^{-1}). In spite of low conductivity of CPES-100 membrane, its extremely low methanol permeability and comparable DMFC polarization characteristics revealed their potential applications to substitute N117 membrane.

The reported procedure for cross-linking of sulfonated aromatic polymers with sulfonated diamine proved to be an effective method to compensate the loss of membrane functionality due to cross-linking. Furthermore, reported cross-linking process may be a cost effective tool for the development highly functionalized cross-linked aromatic polymer membranes as suitable substitute of N117 membrane for diversified fuel cell and electro-membrane applications.

Acknowledgements

Financial assistance received from Department of Science and Technology, New Delhi (Govt. of India) by sponsoring project no. SR/S1/PC/06/2008 is gratefully acknowledged. Instrumental support received from Analytical Science Division, CSMCRI is also gratefully acknowledged. BPT is grateful to CSIR, Govt. of India for award of SRF.

References

1 T. J. Peckham, J. Schmeisser and S. Holdcroft, *J. Phys. Chem. B*, 2008, **112**, 2848.
2 B. J. Liu, G. P. Robertson, D. S. Kim, M. D. Guiver, W. Hu and Z. H. Jiang, *Macromolecules*, 2007, **40**, 1934.
3 K. Miyatake, Y. Chikashige, E. Higuchi and M. Watanabe, *J. Am. Chem. Soc.*, 2007, **129**, 3879.
4 F. Barbir and S. Yazici, *Int. J. Energy Res.*, 2008, **32**, 369.
5 Q. Li, R. He, J. O. Jensen and N. J. Bjerrum, *Chem. Mater.*, 2003, **15**, 4896.
6 O. Savadogo, *J. Power Sources*, 2004, **127**, 135.
7 J. Roziere and D. J. Jones, *Annu. Rev. Mater. Res.*, 2003, **33**, 503.
8 Y. Sone, P. Ekdunge and D. Simonsson, *J. Electrochem. Soc.*, 1996, **143**, 1254.
9 J. J. Sumner, S. E. Creager, J. J. Ma and D. D. Desmarteau, *J. Electrochem. Soc.*, 1998, **145**, 107.
10 P. Costamagna and S. Srinivasan, *J. Power Sources*, 2001, **102**, 242.
11 M. A. Hickner, H. Ghassemi, Y. S. Kim, B. R. Einsla and J. E. McGrath, *Chem. Rev.*, 2004, **104**, 4587.
12 M. S. Kang, J. H. Kim, J. Won, S. H. Moon and Y. S. Kang, *J. Membr. Sci.*, 2005, **247**, 127.
13 B. P. Ladewig, R. B. Knott, A. J. Hill, J. D. Riches, J. W. White, D. J. Martin, J. C. Diniz da costa and G. Q. Lu, *Chem. Mater.*, 2007, **19**, 2372.
14 M. K. Ravikumar and A. K. Shukla, *J. Electrochem. Soc.*, 1996, **143**, 2601.
15 F. Wang, M. Hickner, Y. S. Kim, T. A. Zawodzinski and J. E. McGrath, *J. Membr. Sci.*, 2002, **197**, 231.
16 B. P. Tripathi and V. K. Shahi, *J. Colloid Interface Sci.*, 2007, **316**, 612.
17 B. P. Tripathi, M. Kumar and V. K. Shahi, *J. Membr. Sci.*, 2009, **327**, 145.
18 Y. Á. Gallego, S. P. Nunes, A. E. Lozano, J. G. Campa and J. Abajo, *Macromol. Rapid Commun.*, 2007, **28**, 616.
19 J. H. Fang, X. X. Guo, S. Harada, T. Watari, K. Tanaka, H. Kitan and K. Okamoto, *Macromolecules*, 2002, **35**, 9022.
20 N. Asano, M. Aoki, S. Suzuki, K. Miyatake, H. Uchida and M. Watanabe, *J. Am. Chem. Soc.*, 2006, **128**, 1762.
21 K. Miyatake and M. Watanabe, *J. Mater. Chem.*, 2006, **16**, 4465.
22 M. A. Hofmann, C. M. Ambler, A. E. Maher, E. Chalkova, X. Y. Zhou, S. N. Lvov and H. R. Allcock, *Macromolecules*, 2002, **35**, 6490.
23 M. B. Gieselman and J. R. Reynolds, *Macromolecules*, 1992, **25**, 4832.
24 C. H. Fujimoto, M. A. Hickner, C. J. Cornelius and D. A. Loy, *Macromolecules*, 2005, **38**, 5010.
25 J. Jouanneau, R. Mercier, L. Gonon and G. Gebel, *Macromolecules*, 2007, **40**, 983.
26 C. H. Lee, H. B. Park, Y. S. Chung, Y. M. Lee and B. D. Freeman, *Macromolecules*, 2006, **39**, 755.
27 J. Kerres, W. Zhang and T. Haering, *J. New Mater. Electrochem. Syst.*, 2004, **7**, 299.
28 J. Kerres, A. Ullrich, T. Haring, M. Baldauf, U. Gebhardt and W. Preidel, *J. New Mater. Electrochem. Syst.*, 2000, **3**, 229.
29 J. Kerres, A. Ullrich, F. Meier and T. Haring, *Solid State Ionics*, 1999, **125**, 243.
30 S. D. Mikhailenko, K. P. Wang, S. Kaliaguine, P. X. Xing, G. P. Robertson and M. D. Guiver, *J. Membr. Sci.*, 2004, **233**, 93.
31 S. D. Mikhailenko, G. P. Robertson, M. D. Guiver and S. Kaliaguine, *J. Membr. Sci.*, 2006, **285**, 306.
32 R. Nolte, K. Ledjeff, M. Bauer and R. Mülhaupt, *J. Membr. Sci.*, 1993, **83**, 211.
33 M. Han, G. Zhang, K. Shao, H. Li, Y. Zhang, M. Li, S. Wang and H. Na, *J. Mater. Chem.*, 2010, **20**, 3246.
34 J. Khan, B. P. Tripathi, A. Saxena and V. K. Shahi, *Electrochim. Acta*, 2007, **52**, 6719.
35 Y. Zhang, H. Zhang, X. Zhu and C. Bi, *J. Phys. Chem. B*, 2007, **111**, 6391.
36 B. P. Tripathi and V. K. Shahi, *J. Phys. Chem. B*, 2008, **112**, 15678.
37 B. P. Tripathi and V. K. Shahi, *ACS Appl. Mater. Interfaces*, 2009, **1**, 1002.
38 T. Y. Liu, S. Y. Chen, Y. L. Lin and D. M. Liu, *Langmuir*, 2006, **22**, 9740.
39 A. Saxena, B. P. Tripathi and V. K. Shahi, *J. Phys. Chem. B*, 2007, **111**, 12454.
40 B. P. Tripathi, A. Saxena and V. K. Shahi, *J. Membr. Sci.*, 2008, **318**, 288.
41 G. Socrates, *Infrared Characteristic Group Frequencies*, John Wiley & Sons, Chichester, 1980.
42 T. Uno, K. Machida and K. Hanai, *Chem. Pharm. Bull.*, 1966, **14**, 756.
43 H. Li, Z. Cui, C. Zhao, J. Wu, T. Fu, Y. Zhang, K. Shao, H. Zhang, H. Na and W. Xing, *J. Membr. Sci.*, 2009, **343**, 164.
44 D. B. Spry, A. Goun, K. Glusac, D. E. Moilanen and M. D. Fayer, *J. Am. Chem. Soc.*, 2007, **129**, 8122.
45 M. Saito, N. Arimura, K. Hayamizu and T. Okada, *J. Phys. Chem. B*, 2004, **108**, 16064.
46 M. Eikerling, A. A. Kornyshev and U. Stimming, *J. Phys. Chem. B*, 1997, **101**, 10807.
47 X. B. Zhu, H. M. Zhang, Y. Zhang, Y. M. Liang, X. L. Wang and B. L. Yi, *J. Phys. Chem. B*, 2006, **110**, 14240.
48 A. Siu, J. Schmeisser and S. Holdcraft, *J. Phys. Chem. B*, 2006, **110**, 6072.
49 K. D. Kreuer, *J. Membr. Sci.*, 2001, **185**, 29.

